Mathematical Problems in Engineering
Volume 5, pp. 139–160
Reprints available directly from the publisher
Photocopying permitted by license only

A Model of Frontal Polymerization Using Complex Initiation

P.M. GOLDFEDER and V.A. VOLPERT*,†

Department of Engineering Sciences and Applied Mathematics, Northwestern University, Evanston, IL 60208, USA

(Received 19 May 1998)

Frontal polymerization is a process in which a spatially localized reaction zone propagates into a monomer, converting it into a polymer. In the simplest case of free-radical polymerization, a mixture of monomer and initiator is placed in a test tube. A reaction is then initiated at one end of the tube. Over time, a self-sustained thermal wave, in which chemical conversion occurs, is produced. This phenomenon is possible because of the highly exothermic nature of the polymerization reactions.

Though there are certain advantages to this polymerization process over the more traditional methods, one of the drawbacks is that conversion tends to be incomplete. One way to increase conversion is by using greater amounts of initiator. The disadvantage to using this method is that more initiator results in the production of more free radicals, leading to large numbers of undesirably short polymer chains. A second method is to use a mixture of unstable and stable initiators. In this paper we develop and study a mathematical model of the propagation of free-radical polymerization fronts using such a complex initiation. We compare the propagation velocity, maximum temperature and degree of conversion of fronts with a stable initiator, an unstable initiator and a mixture of the two. In addition, we examine how altering the stability of the stable initiator affects these quantities. We show that it is indeed the case that a mixture of unstable and stable initiators does have many advantages over using either type of initiator individually, in agreement with the existing experimental data.

Keywords: Frontal polymerization; Mathematical modeling

AMS Classification: 80A30, 80A20, 35K57, 34E99

* Corresponding author. Tel.: 847-491-5396. Fax: 847-491-2178.
E-mail: v-volpert@nwu.edu.

†Supported by N.S.F. Grant DMS-9600103.

INTRODUCTION

Frontal polymerization is a process in which a spatially localized reaction zone propagates into a monomer, converting it into a polymer. In the simplest case of free-radical polymerization, a mixture of monomer and initiator is placed in a test tube. A reaction is then initiated at one end of the tube. Over time, a self-sustained thermal wave, in which chemical conversion occurs, is produced. This phenomenon is possible because of the highly exothermic nature of the polymerization reactions.

These reactions will continue to occur until one of two things happens: either complete consumption of the initiator or complete conversion of the monomer. One of the problems which commonly occurs with free-radical polymerization fronts is that the process is truncated for the former reason, and not the latter. This is known as *initiator burnout* [2]. For frontal polymerization to be a viable alternative to more traditional methods, it is necessary for conversion to be at, or near, one-hundred percent.

There are many extremely desirable characteristics of this novel method of creating polymers. Included amongst them is a savings in energy costs, a shorter reaction time, the use of more simple production equipment and improved product purity. One drawback is the aforementioned problem of initiator burnout, which results in incomplete conversion. Thus, the issue is discovery of a way to increase conversion without seriously compromising any of the advantages. One way to do this is by using a larger amount of a single initiator, another way is to use a smaller total amount of two initiators. Because the former method has undesirable side effects, including the production of short polymer chains, we will focus on the latter approach. Unfortunately, there has been very little research done on this.

The idea behind using two initiators is intuitively simple: mix a stable initiator with an unstable one. The advantages of the unstable initiator include a lower activation energy (this allows for initiation at a fairly low temperature) and a higher propagation velocity. Aside from the advantage of a much higher degree of conversion, using a stable initiator also increases the maximum temperature, leading to greater product purity and less waste. A problem with using a stable initiator is that because of its high activation energy it is very difficult

to initiate a self-sustained thermal wave. A second potential problem relates to what was discussed in one of our earlier papers [5], namely heat-loss and the so-called extinction limit. Briefly, what we showed was that for heat losses beyond a certain critical value the wave can no longer propagate. For a very stable initiator, the propagation speed tends to be much lower, which effectively allows for greater amounts of heat loss. One way to circumvent this difficulty in initiation, as well as potential heat-loss problems, is by combining the stable initiator with an easily ignitible unstable one. It has been shown experimentally [10,11] that combining stable and unstable initiators does indeed increase the conversion and maximum temperature, without sacrificing easy initiation, allowing for critical amounts of heat loss, substantially decreasing the speed of the front, or having adverse effects on the size of the polymer chains being produced.

In this paper we develop and study a mathematical model of the propagation of free-radical polymerization fronts using complex initiation. We compare the propagation velocity, maximum temperature and degree of conversion of fronts with a stable initiator, an unstable initiator and a mixture of the two. In addition, we examine how altering the stability of the stable initiator affects these quantities. Comparisons are made between our analytic results and the existing experimental data.

II MATHEMATICAL MODEL

The propagation of free radical polymerization fronts involves the usual free-radical mechanism [7] consisting of decomposition, initiation, propagation and termination reactions. For the process studied in this paper, the characteristic scale of the polymerization wave is much smaller than the vessel through which it propagates, so that the test vessel (usually a test tube) can be treated as infinite on the scale of the polymerization wave. To study polymerization waves that propagate at a constant speed and do not change their profile in the course of propagation, we introduce a moving coordinate system attached to the wave, in which the wave is a stationary solution. Thus a traveling wave coordinate (x) may be introduced. At one side of the vessel ($x=-\infty$) there is a fresh mixture of monomer and initiator, and on

the other side ($x=\infty$) there is the inactive polymer, or products, that are left behind in the wave's wake. The kinetic equations describing this system are written as

$$uI_1' + k_{d1}I_1 = 0, \tag{2.1}$$

$$uI_2' + k_{d2}I_2 = 0, \tag{2.2}$$

$$uR' - 2f_1k_{d1}I_1 - 2f_2k_{d2}I_2 + k_pRM + k_tR\dot{P} = 0, \tag{2.3}$$

$$uM' + k_pRM + k_pM\dot{P} = 0, \tag{2.4}$$

$$u\dot{P}' - k_pRM + k_tR\dot{P} + k_t\dot{P}^2 = 0, \tag{2.5}$$

$$uP' - k_tR\dot{P} - k_t\dot{P}^2 = 0, \tag{2.6}$$

where u is the propagation velocity of the wave which must be determined in the course of solution of the problem. Here I_1, I_2, R, M, and P denote the concentrations in mol/L of the initiators (unstable and stable respectively), primary free radicals, monomer, and inactive polymer, $\dot{P}$ is the concentration of the polymer radicals, and prime denotes the derivative with respect to x. The quantities k_{d1}, k_{d2}, k_p, and k_t are the rate constants for the decomposition, propagation, and termination reactions, respectively, that are all taken in the form of Arrhenius exponentials

$$k_{dn} = k_{dn}^0 \exp(-E_{dn}/R_gT) \quad (n = 1, 2),$$
$$k_p = k_p^0 \exp(-E_p/R_gT), \quad k_t = k_t^0 \exp(-E_t/R_gT),$$

where R_g is the gas constant, T is the temperature of the mixture, and k_{dn}^0, k_p^0, k_t^0 and E_{dn}, E_p, E_t are the frequency factors and activation energies of the three types of reactions.

Equations (2.1) and (2.2) describe the decomposition of the initiators. Here f_1 and f_2 are efficiency factors which are necessary to account for the fact that not all of the radicals produced survive to initiate polymer chains. Equation (2.3) describes both the production (the $2f_1k_{d1}I_1$ and $2f_2k_{d2}I_2$ terms) and consumption (the k_pRM and $k_tR\dot{P}$ terms) of the free radicals. These radicals are produced in the initiator decomposition reactions and consumed in the propagation and termination reactions. In a similar way, the remaining equations (2.4)–(2.6) describe the change in the concentration of the monomer, polymer radicals and inactive polymer, respectively.

These kinetic equations must be supplemented by the energy balance in the system, which accounts for thermal diffusion and heat release in the polymerization process. Since the heat release occurs mainly in the propagation step [9], the energy balance takes the form

$$\kappa T'' - uT' + qk_p(RM + M\dot{P}) = 0, \tag{2.7}$$

where κ is the thermal diffusivity of the mixture (assumed to be constant), and q is the increase in temperature associated with converting 1 mol/L of monomer into polymer.

We will study a simplified kinetic system by using a quasi-steady state assumption regarding the total concentration of the radicals. Under this assumption [3,8], the rate of change of the concentration of the radicals, R and $\dot{P}$, is much smaller than the rates of their production and consumption, so that there is a simple algebraic balance between the amounts of radical and initiator. Thus, equations (2.3)–(2.5) can be reduced to a single equation:

$$uM' + k_{\text{eff}}\sqrt{1 + \hat{f}\frac{k_{d2}}{k_{d1}}\hat{I}}\sqrt{I_1}M = 0, \tag{2.8}$$

where the effective rate constant, k_{eff}, ratio of initiator concentrations, $\hat{I}$, and ratio of efficiency factors, $\hat{f}$, are given by

$$k_{\text{eff}} = k_p\sqrt{2f_1\frac{k_{d1}}{k_t}}, \quad \hat{I} = \frac{I_2}{I_1}, \quad \hat{f} = \frac{f_2}{f_1}.$$

Thus, our model consists of the mass and energy balances (2.1), (2.2), (2.7), and (2.8), and the boundary conditions at the left ($x = -\infty$) and right ($x = \infty$) ends of the tube. For calculational simplicity, we make a change of variables for the initiators, $I_n = J_n^2$ ($n = 1, 2$), and for convenience write the modified equations as

$$uJ_1' + J_1k_1(T) = 0, \tag{2.9}$$

$$uJ_2' + J_2k_3(T) = 0, \tag{2.10}$$

$$uM' + J_1M\sqrt{1 + \hat{f}\frac{k_3(T)}{k_1(T)}\hat{J}^2}k_2(T) = 0, \tag{2.11}$$

$$\kappa T'' - uT' - quM' = 0, \tag{2.12}$$

and the boundary conditions at the cold ($x=-\infty$) and hot ($x=+\infty$) boundaries

$$\begin{aligned} &x=-\infty: \quad M=M_0,\ T=T_0,\ J_n=J_{0n}\ (n=1,2)\\ &x=+\infty: \quad T'=0. \end{aligned} \tag{2.13}$$

Here T_0 is the initial temperature, $J_{0n}=\sqrt{I_{0n}}$ $(n=1,2)$, and M_0 are the amount of (modified) initiators and monomer present in the initial mixture, and

$$\begin{aligned} &k_1(T)=k_{d1}(T)/2=k_{01}\exp(-E_1/R_gT), \quad k_{01}=k_{d1}^0/2,\ E_1=E_{d1},\\ &k_2(T)=k_{eff}(T)=k_{02}\exp(-E_2/R_gT), \quad k_{02}=k_{eff}^0,\ E_2=E_{eff},\\ &k_3(T)=k_{d2}(T)/2=k_{03}\exp(-E_3/R_gT), \quad k_{03}=k_{d2}^0/2,\ E_3=E_{d2}, \end{aligned}$$

where

$$k_{eff}^0=k_p^0\sqrt{2f_1\frac{k_{d1}^0}{k_t^0}}, \quad E_{eff}=E_p+\frac{E_{d1}-E_t}{2}.$$

With the reaction rates in the form of Arrhenius exponentials, this problem is quite difficult to study analytically. In previous works [4–6] the authors of this paper have circumvented this complexity by replacing the Arrhenius dependence of the reaction rates on temperature, $k_n(T)$ $(n=1,2,3)$, by step functions with heights equal to the maximum of the Arrhenius function and integral values over the range T_0 to T_b being approximately equal to those of the Arrhenius functions. This approach has proven to provide results that are not only correct qualitatively, but also quantitatively. Thus we approximate $k_n(T)$ as

$$k_n(T)\approx\begin{cases}0, & T<T_n\\ A_n(T_b), & T>T_n\end{cases}\ (n=1,2,3), \tag{2.14}$$

where

$$T_n=T_b(1-\epsilon_n),\ \epsilon_n=R_gT_b/E_n, \quad A_n(T_b)=k_n(T_b)\ (n=1,2,3). \tag{2.15}$$

Here, T_n $(n=1,2,3)$ are the temperatures at which the reactions begin, ϵ_n are small dimensionless parameters, A_1, A_2, and A_3 are the heights

of the step functions, and $k_1(T_b)$, $k_2(T_b)$, and $k_3(T_b)$ are the reaction rates evaluated at the maximum temperature, T_b. For the subsequent asymptotic analysis, it is important to note that ϵ_1, ϵ_2, and ϵ_3 are of the same order.

Since the typical situation is that the activation energy for the first decomposition reaction, E_1, is greater than that for the polymerization reaction, E_2, formally it is possible for the polymerization reaction to occur prior to the first decomposition reaction which is not consistent with the nature of this model. In order to make up for this inaccuracy of the steady state approximation, we introduce the Heaviside function, $\chi(J_{10} - J_1)$, in the polymerization reaction, rewriting Eqs. (2.11) and (2.12) as

$$uM' + J_1 M \chi(J_{10} - J_1)\sqrt{1 + \hat{f}\frac{A_3(T)}{A_1(T)}\hat{J}^2 A_2(T)} = 0, \tag{2.16}$$

$$\kappa T'' - uT' - quM' = 0. \tag{2.17}$$

Thus, the first decomposition reactions and the polymerization reaction will begin simultaneously as a result of the Heaviside function, χ. Since the set of equations is invariant under spatial translation, we let the point in space where both reactions begin be $x = 0$. Because we have replaced the Arrhenius-type reaction rates with step functions, the spatial region from $x = -\infty$ to $x = +\infty$ can be divided into three regions: one where neither reaction has begun ($x < 0$, $k_1(T) = k_2(T) = k_3(T) = 0$), one in which the first decomposition and the polymerization reactions are occurring but the second initiator has not yet begun to decompose ($0 < x < x_3$, $k_1(T)k_2(T) \neq 0$, $k_3(T) = 0$), and one after the second initiator has begun to decompose ($x > x_3$, $k_1(T)k_2(T)k_3(T) \neq 0$). Thus Eqs. (2.9), (2.10), (2.16), and (2.17) can be stated for each of the three regions as

$$uJ_1' = 0, \quad uJ_2' = 0, \quad uM' = 0, \quad \kappa T'' - uT' = 0, \tag{2.18}$$

for $x < 0$,

$$\begin{aligned} &uJ_1' + J_1(x)A_1 = 0, \quad uJ_2' = 0, \quad uM' + J_1(x)M(x)A_2 = 0, \\ &\kappa T'' - uT' - quM' = 0, \end{aligned} \tag{2.19}$$

for $0 < x < x_3$, and

$$uJ_1' + J_1(x)A_1 = 0, \quad uJ_2' + J_2(x)A_3 = 0,$$
$$uM' + \sqrt{1 + \hat{f}\frac{A_3}{A_1}\hat{J}^2}A_2J_1(x)M(x) = 0, \tag{2.20}$$
$$\kappa T'' - uT' - quM' = 0,$$

for $x > x_3$. The boundary conditions are given in (2.13). In addition, there are the following matching conditions at $x = 0$ and $x = x_3$ that constitute continuity of the mass, temperature and temperature gradient distributions in the polymerization wave:

$$J_1(0^-) = J_1(0^+), \quad J_2(0^-) = J_2(0^+), \quad M(0^-) = M(0^+),$$
$$T(0^-) = T(0^+) = T_1, \quad T'(0^-) = T'(0^+), \tag{2.21}$$

$$J_1(x_3^-) = J_1(x_3^+), \quad J_2(x_3^-) = J_2(x_3^+), \quad M(x_3^-) = M(x_3^+),$$
$$T(x_3^-) = T(x_3^+) = T_3, \quad T'(x_3^-) = T'(x_3^+). \tag{2.22}$$

III SOLUTION

Solution of the Eqs. (2.18)–(2.20) subject to the boundary conditions (2.13) and matching conditions (2.21) and (2.22) were found by first solving the equations for $J(x)$ and $M(x)$, and then substituting the results into the equation for $T(x)$. Solving for $J_n(x)$ and $M(x)$ over all of space yields

$$J_1(x) = \begin{cases} J_{10}, & x < 0, \\ J_{10}e^{-(A_1/u)x}, & 0 < x < x_3, \\ J_{10}e^{-(A_1/u)x}, & x > x_3, \end{cases} \tag{3.1}$$

$$J_2(x) = \begin{cases} J_{20}, & x < 0, \\ J_{20}, & 0 < x < x_3, \\ J_{20}e^{-(A_3/u)(x_3 - x)}, & x > x_3, \end{cases} \tag{3.2}$$

and

$$M(x) = \begin{cases} M_0, & x < 0, \\ M_0 \exp[\alpha(e^{-(A_1/u)x} - 1)], & 0 < x < x_3, \\ M_0 \exp[\alpha(e^{-(A_1/u)x_3} - 1)] \exp[\alpha(F(x) - F(x_3))], & x > x_3, \end{cases} \tag{3.3}$$

where

$$F(x) = \frac{A_1}{u}\int_x^\infty \sqrt{1 + \frac{A_3}{A_1}\phi e^{2((A_1-A_3)/u)\tau} e^{-(A_1/u)\tau}}\, d\tau, \tag{3.4}$$

and the following nondimensional quantities were introduced

$$\alpha = \frac{A_2 J_{01}}{A_1}, \quad \phi = \hat{f}\hat{J}_0^2 e^{(2A_3/u)x_3}.$$

The concentrations $J_1(x)$, $J_2(x)$, and $M(x)$ of the initiators and the monomer given by Eqs. (3.1)–(3.3) satisfy the conditions of continuity in Eqs. (2.21) and (2.22). Solving the equations for $T(x)$ yields

$$T(x) = T_0 + \frac{qu}{\kappa} e^{(u/\kappa)x}\int_x^\infty (M_0 - M(\tau))e^{-(u/\kappa)\tau}\, d\tau \tag{3.5}$$

which is valid over the entire spatial region and satisfies the condition of the continuity of both the temperature and its gradient from Eqs. (2.21) and (2.22). Here, M is given by Eq. (3.3).

Applying the remaining conditions in (2.13), (2.21), and (2.22) produces the following three equations

$$T_1 - T_0 = \frac{qu}{\kappa}\int_0^\infty (M_0 - M(\tau))e^{-(u/\kappa)\tau}\, d\tau, \tag{3.6}$$

$$T_3 - T_0 = \frac{qu}{\kappa} e^{(u/\kappa)x_3}\int_{x_3}^\infty (M_0 - M(\tau))e^{-(u/\kappa)\tau}\, d\tau, \tag{3.7}$$

$$T_b - T_0 = q(M_0 - M_b), \tag{3.8}$$

where M_b, the amount of monomer remaining when the reactions have ceased, is found by taking the limit as $x \to \infty$ of Eq. (3.3)

$$M_b = M_0 \exp[\alpha(e^{-(A_1/u)x_3} - 1)] \exp[-\alpha F(x_3)]. \tag{3.9}$$

Equation (3.8) was derived by evaluating Eq. (3.5) in the limit as $x \to \infty$ and applying L'Hopital's Rule.

We now have four equations for four unknown quantities x_3, T_b, u, and M_b. Before examining these equations, we will determine the

asymptotics of $F(x)$ given by Eq. (3.4) in small ϵ. Nondimensionalizing this integral gives us

$$F(x) = \int_{\xi}^{\infty} \sqrt{1 + \epsilon\phi e^{2(1-\epsilon)t}} e^{-t}\, dt, \tag{3.10}$$

where

$$\xi = \frac{A_1}{u}x, \quad t = \frac{A_1}{u}\tau, \quad \epsilon = \frac{A_3}{A_1} \ll 1.$$

This can be rewritten as

$$\begin{aligned} F(x) &= \int_{\xi}^{\infty} \sqrt{e^{-2t} + \epsilon\phi e^{-2\epsilon t}}\, dt \\ &= \int_{\xi}^{\infty} \sqrt{\epsilon\phi e^{-2\epsilon t}}\, dt + \int_{\xi}^{\infty} \frac{e^{-2t}}{\sqrt{e^{-2t} + \epsilon\phi e^{-2\epsilon t}} + \sqrt{\epsilon\phi e^{-2\epsilon t}}}\, dt \\ &= \sqrt{\epsilon\phi} \int_{\xi}^{\infty} e^{-\epsilon t}\, dt + \int_{\xi}^{\infty} \frac{e^{-2t}}{\sqrt{e^{-2t} + \epsilon\phi} + \sqrt{\epsilon\phi}}\, dt + I, \end{aligned} \tag{3.11}$$

where

$$I = \int_{\xi}^{\infty} e^{-2t} \left(\frac{1}{\sqrt{e^{-2t} + \epsilon\phi e^{-2\epsilon t}} + \sqrt{\epsilon\phi e^{-2\epsilon t}}} - \frac{1}{\sqrt{e^{-2t} + \epsilon\phi} + \sqrt{\epsilon\phi}} \right) dt.$$

It can be shown that

$$I \le 2\sqrt{\epsilon\phi} \int_{\xi}^{\infty} \frac{\epsilon t}{2\epsilon\phi e^{2t}}\, dt. \tag{3.12}$$

Thus, it is apparent that I is, at most, an $O(\sqrt{\epsilon})$ quantity, which allows for the following approximation for $F(x)$

$$\begin{aligned} F(x) &= \sqrt{\phi/\epsilon}\, e^{-\epsilon(A_1/u)x} + \int_{\xi}^{\infty} \frac{e^{-2t}}{\sqrt{e^{-2t} + \epsilon\phi} + \sqrt{\epsilon\phi}}\, dt + O(\sqrt{\epsilon}) \\ &= \sqrt{\phi/\epsilon}\, e^{-\epsilon(A_1/u)x} + e^{-(A_1/u)x} + O(\sqrt{\epsilon}\ln\epsilon). \end{aligned} \tag{3.13}$$

Inserting this result into Eq. (3.9) allows us to write a simple expression for M_b (in the original variables)

$$M_b = M_0 \exp\left[-\alpha\left(1 + \sqrt{\frac{\hat{f}}{\epsilon}}\hat{J}_0\right)\right] + O(\sqrt{\epsilon}\ln\epsilon). \tag{3.14}$$

Now that an approximate expression for $F(x)$ has been found, it is possible for us to find analytic solutions for Eqs. (3.6)–(3.8). Instead of attempting to solve them in their current form, it will be easier to generate a new set of equations by looking at their differences. First subtracting Eq. (3.6) from Eq. (3.8) gives us

$$\begin{aligned} T_b - T_1 &= \frac{qu}{\kappa}\int_0^\infty [M(\tau) - M_b]e^{-(u/\kappa)\tau}\,d\tau \\ &= \frac{qu}{\kappa}\left(\int_0^{x_3}\left[M_0 e^{\alpha(e^{-(A_1/u)\tau}-1)} - M_b\right]e^{-(u/\kappa)\tau}\,d\tau\right. \\ &\quad \left. + M_b\int_{x_3}^\infty [e^{\alpha F(\tau)} - 1]e^{-(u/\kappa)\tau}\,d\tau\right). \end{aligned} \tag{3.15}$$

Subtracting Eq. (3.7) from Eq. (3.8)

$$\begin{aligned} T_b - T_3 = \frac{qu}{\kappa}\left(\int_0^\infty [M_0 - M_b]e^{-(u/\kappa)\tau}\,d\tau\right. \\ \left. - e^{-(u/\kappa)x_3}\int_{x_3}^\infty [M_0 - M(\tau)]e^{-(u/\kappa)\tau}\,d\tau\right). \end{aligned} \tag{3.16}$$

By adding and subtracting factors of $\int_{x_3}^\infty M(\tau)e^{-(u/\kappa)\tau}\,d\tau$ and $\int_0^{x_3}[M(\tau) - M_b]e^{-(u/\kappa)\tau}\,d\tau$, rearranging and simplifying, Eq. (3.16) can be rewritten as

$$\begin{aligned} T_b - T_3 &= q(M_0 - M_b)(1 - e^{-(u/\kappa)x_3}) + \frac{qu}{\kappa} \\ &\quad \times \left(\int_0^\infty [M(\tau) - M_b]e^{-(u/\kappa)\tau}\,d\tau\right. \\ &\quad - \int_0^{x_3}[M(\tau) - M_b]e^{-(u/\kappa)\tau}\,d\tau - (e^{(u/\kappa)x_3} - 1) \\ &\quad \left. \times \int_{x_3}^\infty [M_0 - M(\tau)]e^{-(u/\kappa)\tau}\,d\tau\right). \end{aligned} \tag{3.17}$$

Substituting in results from Eq. (3.15), adding and subtracting $(e^{(u/\kappa)x_3} - 1)\int_{x_3}^{\infty} M_b e^{-(u/\kappa)\tau}\,d\tau$, and simplifying yields

$$T_1 - T_3 = q(M_0 - M_b)(1 - e^{-(u/\kappa)x_3}) + \frac{qu}{\kappa}\int_0^{x_3} M_b e^{-(u/\kappa)\tau}\,d\tau$$
$$- \frac{qu}{\kappa}(e^{(u/\kappa)x_3} - 1)\left(\int_{x_3}^{\infty}[M_0 - M_b]e^{-(u/\kappa)\tau}\,d\tau\right.$$
$$\left. + \int_{x_3}^{\infty}[M_b - M(\tau)]e^{-(u/\kappa)\tau}\,d\tau\right). \tag{3.18}$$

Simplifying this expression gives us

$$T_1 - T_3 = (T_b - T_1 + qM_b)(e^{(u/\kappa)x_3} - 1)$$
$$- qe^{(u/\kappa)x_3}\frac{u}{\kappa}\int_0^{x_3} M(\tau)e^{-(u/\kappa)\tau}\,d\tau. \tag{3.19}$$

Since reaction zone for this system is known to be quite small, it is reasonable to consider the nondimensional quantity $(u/\kappa)x_3$ as an $O(\epsilon_n)$ quantity. Using this assumption, as well as the fact that the quantity $(T_b - T_1)/T_b$ is also an $O(\epsilon_n)$ quantity $(n = 1, 2, 3)$, we can rewrite Eq. (3.19) to $O(\epsilon_n)$ as

$$T_1 - T_3 = qM_b\frac{u}{\kappa}x_3 - q\frac{u}{\kappa}\int_0^{x_3} M(\tau)e^{-(u/\kappa)\tau}\,d\tau. \tag{3.20}$$

Adding this result to Eq. (3.15) and again taking advantage of $(u/\kappa)x_3$ being $O(\epsilon_n)$ gives us to $O(\epsilon_n)$

$$T_b - T_3 = qM_b\frac{u}{\kappa}\int_{x_3}^{\infty}[e^{\alpha F(\tau)} - 1]e^{-(u/\kappa)\tau}\,d\tau. \tag{3.21}$$

Thus, we now have the four equations (3.8), (3.14), (3.20), and (3.21) for the four unknown quantities T_b, M_b, u, and x_3. We rewrite the

equations here for convenience

$$T_b - T_0 = q(M_0 - M_b), \tag{3.22}$$

$$M_b = M_0 \exp\left[-\alpha\left(1 + \sqrt{\frac{\hat{f}}{\epsilon}}\hat{J}_0\right)\right], \tag{3.23}$$

$$T_1 - T_3 = qM_b\frac{u}{\kappa}x_3 - q\frac{u}{\kappa}\int_0^{x_3} M(\tau)e^{-(u/\kappa)\tau}\,d\tau, \tag{3.24}$$

$$T_b - T_3 = qM_b\frac{u}{\kappa}\int_{x_3}^{\infty}[e^{\alpha F(\tau)} - 1]e^{-(u/\kappa)\tau}\,d\tau, \tag{3.25}$$

where

$$F(x) = \hat{J}_0\sqrt{\frac{\hat{f}}{\epsilon}}e^{-\epsilon(A_1/u)(x-x_3)} + e^{-(A_1/u)x}.$$

Note that the latter four equations are of $O(\epsilon_n)$. Substituting results from Eq. (3.3) into the integral in Eq. (3.24) yields

$$T_1 - T_3 \approx qM_b\frac{u}{\kappa}x_3 - qM_0e^{-\alpha}\int_0^{\xi_0}\exp[\alpha e^{-(v/\alpha)t}]e^{-t}\,dt, \tag{3.26}$$

where

$$t = \frac{u}{\kappa}\tau, \quad \xi_0 = \frac{u}{\kappa}x_3, \quad v = \frac{\kappa A_2 J_{01}}{u^2}.$$

This can be rewritten as

$$\begin{aligned} T_1 - T_3 &\approx qM_b\frac{u}{\kappa}x_3 - qM_0e^{-\alpha}\frac{\alpha}{v}\int_{e^{-(v/\alpha)\xi_0}}^{1} e^{\alpha y}y^{(\alpha/v)-1}\,dy \\ &\approx qM_b\frac{u}{\kappa}x_3 - qM_0e^{-\alpha}\left(\xi_0\exp[\alpha e^{-(v/\alpha)\xi_0}]\right. \\ &\quad \left. -\frac{\alpha^2}{v}\int_{e^{-(v/\alpha)\xi_0}}^{1} e^{\alpha y}\ln y\,dy\right), \end{aligned} \tag{3.27}$$

where we again took advantage of ξ_0 being a small quantity and, in addition, assumed (as in our previous paper [4]) that due to a large

activation energy, $\alpha/\nu \ll 1$. This equation can be rewritten as

$$(\epsilon_3 - \epsilon_1)\frac{T_b}{qM_0}e^{\alpha} \approx \xi_0\left(\exp\left[-\alpha\hat{J}_0\sqrt{\frac{\hat{f}}{\epsilon}}\right] - \exp[\alpha e^{-(\nu/\alpha)\xi_0}]\right) + \frac{\alpha^2}{\nu}\int_{e^{-(\nu/\alpha)\xi_0}}^{1} e^{\alpha y}\ln y\,dy. \tag{3.28}$$

Turning our attention to the integral in Eq. (3.25), we again begin by nondimensionalizing it, which yields

$$qM_b\int_{\xi_0}^{\infty}(\exp[\alpha(\eta e^{-\epsilon(\nu/\alpha)t} + e^{-(\nu/\alpha)t})] - 1)e^{-t}\,dt = qM_b\left(1 - e^{-\xi_0} + \int_0^{e^{-\xi_0}}\exp[\alpha\eta y^{(\epsilon\nu/\alpha)} + \alpha y^{(\nu/\alpha)}]\,dy\right), \tag{3.29}$$

where

$$\eta = \hat{J}_0\sqrt{\frac{\hat{f}}{\epsilon}}e^{\epsilon(\nu/\alpha)\xi_0}.$$

Though the integral in this equation cannot readily be solved analytically, using the fact that $\eta \gg 1$ (we are assuming that $\hat{J}_0$ will not be a small quantity, i.e., a substantial amount of the stable initiator is present in the initial mixture), we can approximate it using Laplace's method (see, for example, [1]) as

$$\frac{1}{\epsilon\eta\nu}\exp\left[\frac{\epsilon\nu}{\alpha}\xi_0 - \xi_0 + \alpha e^{-(\nu/\alpha)\xi_0} + \alpha\eta e^{-(\epsilon\nu/\alpha)\xi_0}\right].$$

Substituting in for η and expanding all of the exponentials (assuming that $(\epsilon\nu/\alpha)\xi_0$ is a small quantity) allows us to rewrite the integral as

$$\frac{1}{\hat{J}_0\sqrt{\hat{f}\epsilon\nu}}[1 - \xi_0 + \cdots]\left[1 - \frac{\epsilon\nu}{\alpha}\xi_0 + \cdots\right]\left[1 + \frac{\epsilon\nu}{\alpha}\xi_0 + \cdots\right] \times \exp\left[\alpha\left(\hat{J}_0\sqrt{\frac{\hat{f}}{\epsilon}} + e^{-(\nu/\alpha)\xi_0}\right)\right]. \tag{3.30}$$

Substituting this result back into Eq. (3.29), neglecting $e^{-(\nu/\alpha)\xi_0}$ compared to $\hat{J}_0\sqrt{\hat{f}/\epsilon}$ within the exponential, and keeping only terms to $O(\epsilon)$ yields

$$qM_b\left(\xi_0+\frac{1}{\hat{J}_0\nu\sqrt{\hat{f}\epsilon}}\exp\left[\alpha\hat{J}_0\sqrt{\frac{\hat{f}}{\epsilon}}\right]\right). \tag{3.31}$$

Using the approximation for M_b from Eq. (3.23), substituting these results into Eq. (3.25) and simplifying gives us the following equation

$$\xi_0\exp\left[-\alpha\hat{J}_0\sqrt{\frac{\hat{f}}{\epsilon}}\right]\approx\frac{\epsilon_3 T_b}{qM_0}e^{\alpha}-\frac{1}{\hat{J}_0\nu\sqrt{\hat{f}\epsilon}}. \tag{3.32}$$

The left-hand side of this equation consists of an exponentially small term multiplied by a small quantity. Thus, it would be reasonable to say that the two terms on the right-hand side can be considered as being very nearly equal to one another. This gives an approximate equation for ν, the nondimensional propagation speed,

$$\nu\approx\left(\hat{J}_0\sqrt{\hat{f}\epsilon}\frac{\epsilon_3 T_b}{qM_0}e^{\alpha}\right)^{-1}. \tag{3.33}$$

Using the definitions of ν and ϵ_3 given above allows us to write an equation for the dimensional propagation velocity

$$u^2=\frac{\kappa A_2 R_g T_b^2 J_{02} e^{\alpha}}{E_3 qM_0}\sqrt{\hat{f}\frac{A_3}{A_1}}, \tag{3.34}$$

which can be rewritten in the original variables as

$$u^2=\frac{\kappa R_g T_b^2}{E_{d2}qM_0}k_p^0\sqrt{2f_2 I_{02}\frac{k_{d2}^0}{k_t^0}}\exp\left[\frac{E_t-E_{d2}-2E_p}{2R_g T_b}\right]$$
$$\times\exp\left[2k_p^0\sqrt{\frac{I_{01}}{k_{d1}^0 k_t^0}}\exp\left[\frac{E_t+E_{d1}-2E_p}{2R_g T_b}\right]\right]. \tag{3.35}$$

If T_b is fairly close to the adiabatic temperature, T_{ad} (which is the case if M_b is small), then this is an explicit formula for the propagation

velocity. Otherwise, combining it with Eqs. (3.22) and (3.23) and solving it numerically (as we do below) is necessary.

IV RESULTS

Examining Eqs. (3.22), (3.23), and (3.35) numerically, we were able to observe how changes in the initiator type and composition affected the maximum temperature in the front (T_b), the final degree of conversion of the monomer (M_b), and the propagation velocity (u).

Unless otherwise noted, the following parameter values were used [4,10]:

$$\begin{aligned} &k_{d1}^0 = 4 \cdot 10^{12}\,1/\mathrm{s}, && k_p^0 = 5 \cdot 10^6\,\mathrm{L}/(\mathrm{s}\cdot\mathrm{mol}), && k_t^0 = 3 \cdot 10^7\,\mathrm{L}/(\mathrm{s}\cdot\mathrm{mol}),\\ &E_{d1} = 27\,\mathrm{kcal/mol}, && E_p = 4.7\,\mathrm{kcal/mol}, && E_t = 0.7\,\mathrm{kcal/mol},\\ &k_{d2}^0 = 8.9 \cdot 10^{12}\,1/\mathrm{s}, && && E_{d2} = 31.3\,\mathrm{kcal/mol},\\ &q = 33.24\,\mathrm{L}\cdot\mathrm{K/mol}, && && \kappa = 0.0014\,\mathrm{cm}^2/\mathrm{s}. \end{aligned} \tag{4.1}$$

In addition, we fixed the initial temperature (T_0) at 300 K, and the initial amount of monomer present (M_0) at 6 mol/L. In Figs. 1–3, we compare how changes in the type and consistency of the initiator will affect the maximum temperature, amount of monomer remaining and propagation velocity. The quantity I_0 in these figures (as well as Figs. 4–6) denotes the *total* amount of initiator present, whether it is all of one type or a mixture. In the cases where we mixed initiators, the ratio of stable to unstable initiator was one-to-one. For the cases where only a single initiator was used the asymptotics in this paper will not work due to the fact that the parameter $\hat{J}_0$ will either be zero or infinite, making it necessary to use alternate equations for T_b, M_b, and u. In a previous paper [4] we have derived equations for these quantities. We write them here for convenience:

$$\begin{aligned} T_b - T_0 &= q(M_0 - M_b),\\ M_b &= M_0 e^{-\alpha},\\ u^2 &= \frac{\kappa A_1 R_g T_b^2}{E_1 (T_b - T_0)} \frac{e^\alpha - 1}{\alpha \int_0^1 e^{\alpha y} \ln(1/y)\,dy}, \end{aligned}$$

where A_1 and α are defined as in this paper.

Figure 1 is a plot showing the effect of initiator type on the maximum temperature achieved. For the cases of a single initiator, stability tends to radically increase the maximum temperature. This is expected, as the higher activation energy (E_{d2}) characteristic of a more stable initiator means that the temperature must reach a higher value before any significant initiation can occur. Thus, because the reactions are harder to initiate and therefore begin at a higher temperature with a stable initiator, even with a gradient similar to the unstable initiator, a higher maximum temperature will be reached. For the case of a mixture of initiators, the maximum temperature achieved is nearly as high as that for the stable initiator alone for very small amounts of initiator. Though it is not shown on this graph, for slightly higher amounts of initiator, the maximum temperature achieved for the mixed initiators is actually slightly greater than for the stable one only. As was mentioned above, this is a desirable characteristic.

Figure 2 lends even greater validity to the theory of mixing stable and unstable initiators in frontal polymerization. This figure shows the

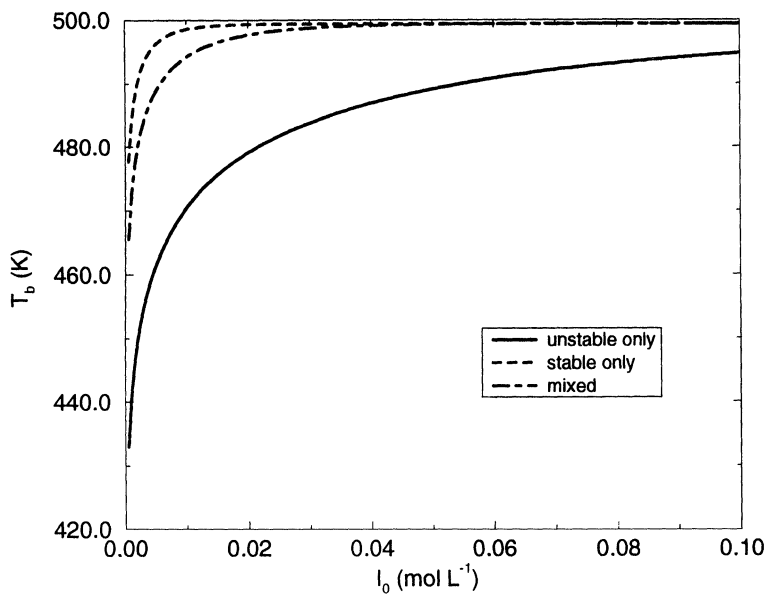

FIGURE 1 Effect of changes in initiator type and composition on the maximum temperature of the system.

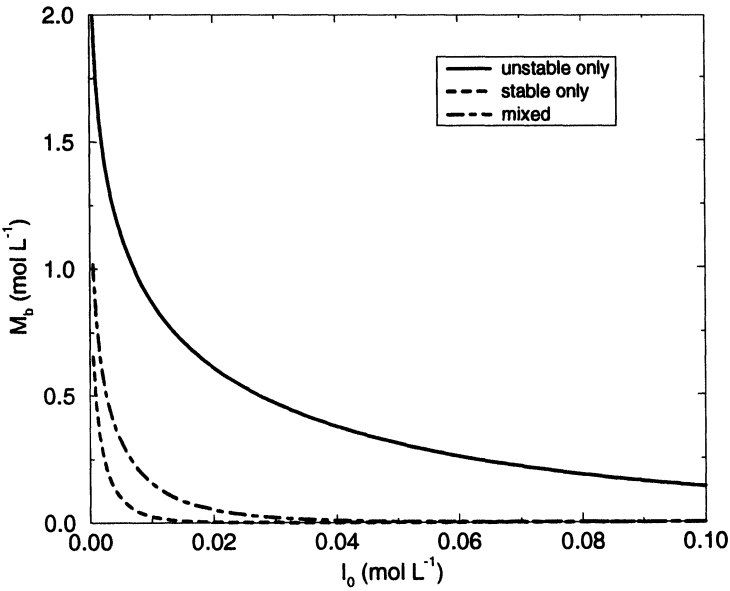

FIGURE 2 Effect of changes in initiator type and composition on the amount of unreacted monomer remaining after the reactions have ceased.

effects of changes in the initiator type and composition on the amount of monomer remaining once the reactions have run to completion shows that for a mixed initiator, conversion is nearly complete for even small amounts of initiator. For a stable initiator only, conversion is slightly higher for smaller amounts of initiator, but for concentrations greater then $0.05\,\text{mol}\,\text{L}^{-1}$ complete conversion is achieved for either a stable or mixed initiator. This is in stark contrast to the unstable initiator, where conversion is never much greater than ninety-five percent.

Figure 3 shows how the front velocity is affected by the type of initiator. As was mentioned above, one of the goals of using two initiators was to increase conversion without decreasing speed. This figure shows that it is indeed not necessary to sacrifice speed for greater conversion. For initiator concentrations greater than $0.010\,\text{mol}\,\text{L}^{-1}$, the velocity for the mixed initiator is greater than that for the stable one. In fact, as can be seen in the graph, as the total amount of initiator increases, the difference between these velocities

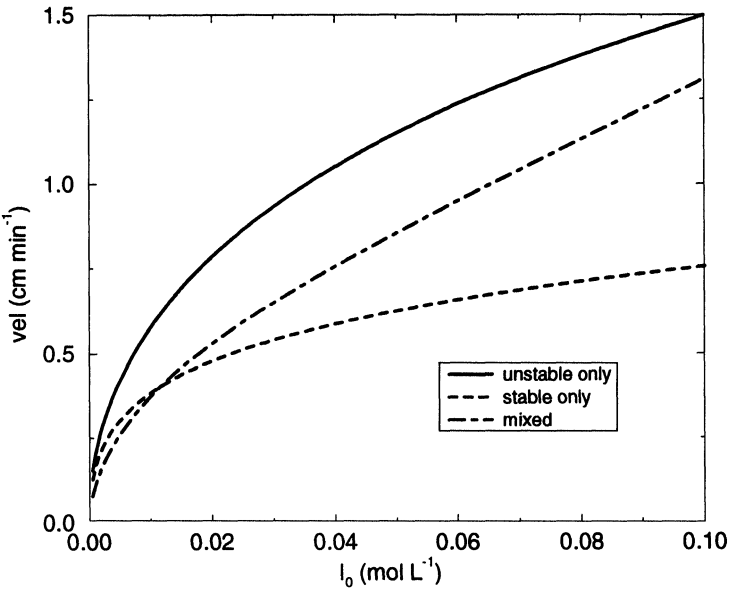

FIGURE 3 Effect of changes in initiator type and composition on the propagation velocity of the front.

increases dramatically. Thus, having a mixed initiator definitely does not result in very much of a loss of speed.

Figures 4–6 show how changing the activation energy of the stable initiator, I_2, affects the maximum temperature, amount of monomer remaining and propagation velocity. The lower the activation energy, the less stable I_2. For these plots, an equal mixture of stable and unstable initiators was used. A less stable I_2 (due to a lower activation energy) tended to produce a lower maximum temperature, lower conversion and higher velocity. The results of Fig. 4 are apparent from looking at the following equation, derived from Eqs. (3.22) and (3.23)

$$\left(\frac{2\sqrt{I_{02}}k_p^0}{\sqrt{k_{d2}^0 k_t^0}}\sqrt{\hat{f}}\right)\exp\left[\frac{E_t + E_{d2} - 2E_p}{2R_g T_b}\right] = \ln\left(\frac{qM_0}{T_0 + qM_0 - T_b}\right)$$

(where it was assumed that, because $1 \ll \sqrt{(\hat{f}/\epsilon)}\hat{J}_0$, the exponential of Eq. (3.23) could be approximated as $-\alpha\sqrt{(\hat{f}/\epsilon)}\hat{J}_0$. As the activation

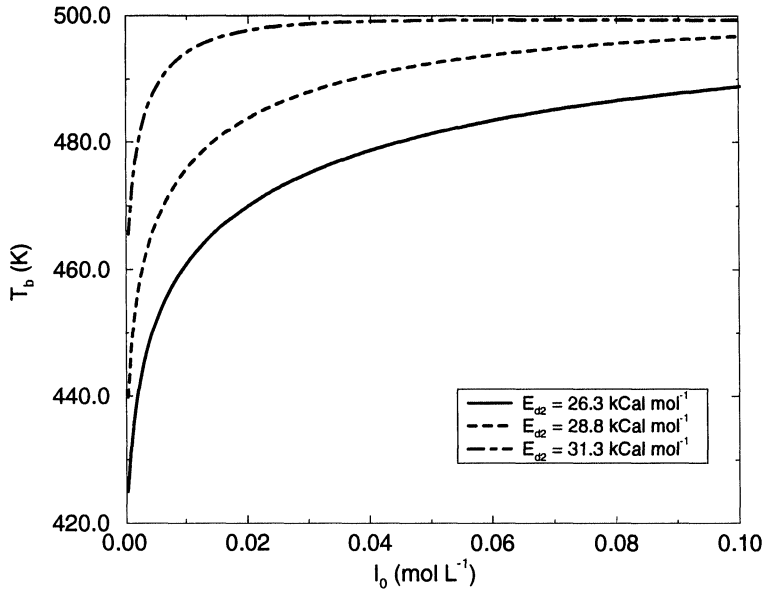

FIGURE 4 Effect of changes in the activation energy of the stable initiator on the maximum temperature of the system.

energy of the stable initiator, E_{d2}, is lowered the value of the left-hand side of this equation decreases. The accompanying decrease in the right-hand side of the equation can only be caused by a decrease in T_b. Figures 5 and 6 can be understood through similar reasoning by examining Eqs. (3.23) and (3.35), respectively.

Comparing our results with the available experimental data [10,11] shows fairly good agreement. These experimental papers show that a more stable initiator causes a higher maximum temperature, lower propagation velocity and much greater conversion than an unstable one, without the undesirably short polymer chains. Specifically, it was shown that the propagation velocity dependence on initiator is not additive, maximum temperatures were higher for an initiator mixture than for either type of initiator alone, and that conversion is (for amounts of initiator that were not too small) nearly equal for mixed and stable initiators. The results of this paper were in excellent qualitative, as well as very good quantitative, agreement with each of these findings.

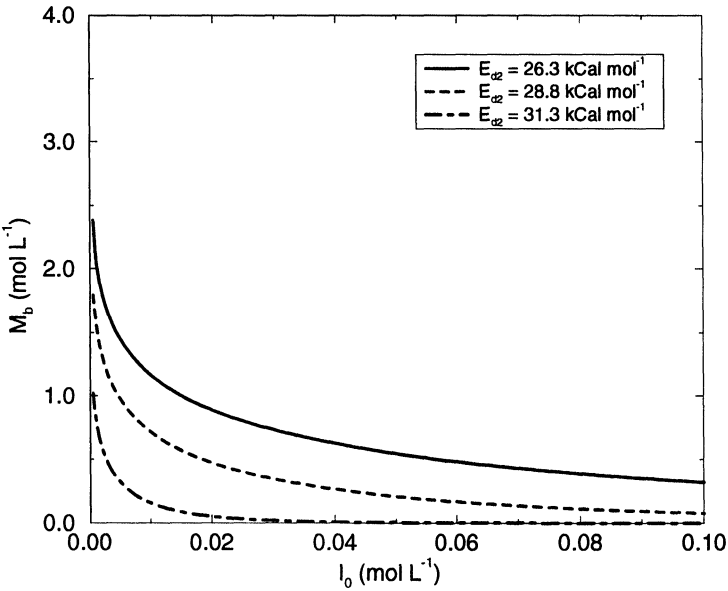

FIGURE 5 Effect of changes in the activation energy of the stable initiator on the amount of unreacted monomer remaining after the reactions have ceased.

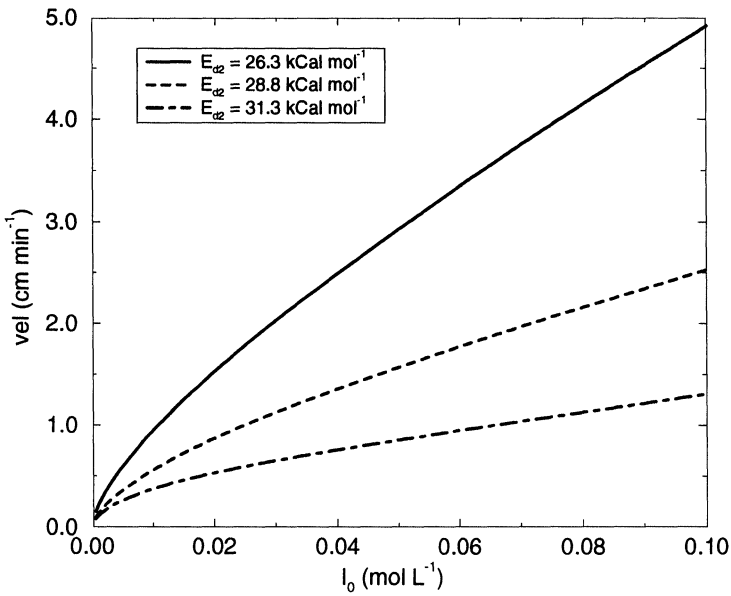

FIGURE 6 Effect of changes in the activation energy of the stable initiator on the propagation velocity of the front.

We have introduced a mathematical model of a free-radical polymerization front using complex initiation. In doing so, we have confirmed that a combination of stable and unstable initiators tends to make this method of polymerization more viable than with a single initiator.

References

[1] C.M. Bender and S.A. Orszag, *Advanced Mathematical Methods for Scientists and Engineers*, McGraw Hill, New York, 1978.
[2] S.P. Davtyan, P.V. Zhirkov and S.A. Vol'fson, Problems of non-isothermal character in polymerization processes, *Russ. Chemical Reviews*, **53** (1984) 150–163.
[3] N.A. Dotson, R. Galvan, R.L. Laurence and M. Tirrell, *Polymerization Process Modeling*, VCH Publishers, New York, 1996.
[4] P.M. Goldfeder, V.A. Volpert, V.M. Ilyashenko, A. Khan, J.A. Pojman and S.E. Solovyov, Mathematical modeling of free radical polymerization fronts, *J. Phys. Chem. B*, **101** (1997), 3474–3482.
[5] P.M. Goldfeder and V.A. Volpert, Nonadiabatic frontal polymerization. *J. Engg. Mathematics*, **34** (1998), 301–318.
[6] P.M. Goldfeder and V.A. Volpert, A mathematical model of frontal polymerization including the gel effect. *Mathematical Problems in Engg.*, **4** (1998), 377–391.
[7] V.R. Gowariker, N.V. Viswanathan and J. Sreedhar, *Polymer Science*, John Wiley and Sons, 1986.
[8] P.C. Hiemenz, Polymer Chemistry, Marcel Dekker, New York, 1984.
[9] G.B. Manelis, L.P. Smirnov and N.J. Peregudov, Nonisothermal kinetics of polymerization processes. *Combustion, Explosion, and Shock Waves*, **13** (1977), 389–393.
[10] J.A. Pojman, J. Willis, D. Fortenberry, V. Ilyashenko and A. Khan, Factors affecting propagating fronts of addition polymerization: velocity, front curvature, temperature profile, conversion and molecular weight distribution, *J. Polymer Sci., Part A: Polymer Chemistry*, **33** (1995), 643–652.
[11] A.O. Tonoyan, Kh.A. Arutyunyan, S.P. Davtyan, B.A. Rozenberg and N.S. Yenikolopyan, Adiabatic polymerization of methyl methacrylate and of styrene using complex initiation, *Vysokomol. Soyed.*, **A16**(4) (1974), 768–771.

Mathematical Problems in Engineering

Special Issue on
Modeling Experimental Nonlinear Dynamics and Chaotic Scenarios

Call for Papers

Thinking about nonlinearity in engineering areas, up to the 70s, was focused on intentionally built nonlinear parts in order to improve the operational characteristics of a device or system. Keying, saturation, hysteretic phenomena, and dead zones were added to existing devices increasing their behavior diversity and precision. In this context, an intrinsic nonlinearity was treated just as a linear approximation, around equilibrium points.

Inspired on the rediscovering of the richness of nonlinear and chaotic phenomena, engineers started using analytical tools from "Qualitative Theory of Differential Equations," allowing more precise analysis and synthesis, in order to produce new vital products and services. Bifurcation theory, dynamical systems and chaos started to be part of the mandatory set of tools for design engineers.

This proposed special edition of the *Mathematical Problems in Engineering* aims to provide a picture of the importance of the bifurcation theory, relating it with nonlinear and chaotic dynamics for natural and engineered systems. Ideas of how this dynamics can be captured through precisely tailored real and numerical experiments and understanding by the combination of specific tools that associate dynamical system theory and geometric tools in a very clever, sophisticated, and at the same time simple and unique analytical environment are the subject of this issue, allowing new methods to design high-precision devices and equipment.

Authors should follow the Mathematical Problems in Engineering manuscript format described at http://www.hindawi.com/journals/mpe/. Prospective authors should submit an electronic copy of their complete manuscript through the journal Manuscript Tracking System at http://mts.hindawi.com/ according to the following timetable:

Manuscript Due	February 1, 2009
First Round of Reviews	May 1, 2009
Publication Date	August 1, 2009

Guest Editors

José Roberto Castilho Piqueira, Telecommunication and Control Engineering Department, Polytechnic School, The University of São Paulo, 05508-970 São Paulo, Brazil; piqueira@lac.usp.br

Elbert E. Neher Macau, Laboratório Associado de Matemática Aplicada e Computação (LAC), Instituto Nacional de Pesquisas Espaciais (INPE), São Josè dos Campos, 12227-010 São Paulo, Brazil ; elbert@lac.inpe.br

Celso Grebogi, Department of Physics, King's College, University of Aberdeen, Aberdeen AB24 3UE, UK; grebogi@abdn.ac.uk